

## Electrical Properties of Copper Phthalocyanine at High Pressure\*

J. RIMAS VAIŠNYS AND R. S. KIRK

*Department of Engineering and Applied Science, Yale University, New Haven, Connecticut*

(Received 23 July 1965)

The electrical properties of copper phthalocyanine were studied over a pressure range extending to 60 000 bars. Discontinuities of the energy gap, thermoelectric power, and resistance indicate the presence of two new phases at high pressure. At 1 atmosphere the activation energy is 0.85 eV; from about 2 to 30 kbar the energy varies between 0.45 and 0.35 eV; after rising to 0.55 eV at 30 kbar, it decreases continuously to 0.50 eV at 60 kbar. At 30 kbar, as pressure is increased, the thermoelectric energy reverses sign, going from +0.3 to -0.3 eV, while the pre-exponential factor in the conductivity expression increases by a factor of 10. The results are analyzed in terms of an energy-band model with deep-lying impurity levels. It is found that at high pressures the activation energy is a direct measure of the energy gap. The 30-kbar transformation is accompanied by order-of-magnitude changes in the carrier mobilities and state densities, suggesting that marked changes in the energy-band structure have occurred. Tight-binding calculations indicate that these changes are due to orientation effects.

### INTRODUCTION

MOLECULES in organic crystals interact only very weakly; the interaction energy per valence electron is of the order of the thermal energy at 300°K. For this reason rates of charge and energy transport through such crystals are low. On the other hand, for related reasons, such crystals are very compressible. Application of pressure can increase the energy of the system by an amount equal to the original interaction energy, resulting in a large change in the coupling between the molecules. In addition, pressure may induce structural transformations, again involving similar energy changes. Thus, by using pressure as a variable it should be possible to study the connection between the basic geometrical parameters, the intermolecular distance or orientation, and charge transport in molecular systems.

LeBlanc<sup>1</sup> has shown that energy states in anthracene crystals can be described by the energy-band approach, and Friedman<sup>2</sup> has derived a number of the transport coefficients for the appropriate narrow bands. Examination of these arguments suggests that the band approach is even more applicable to molecular solids under pressure. Appropriate pressure experiments could serve to verify the applicability of the band model as well as to clarify some of the features which control charge transport in such solids.

The material chosen for this work was copper phthalocyanine (Cu-Phth), whose electrical behavior at 1 atmosphere is well characterized.<sup>3,4</sup> In addition, preliminary work indicated the existence of a pressure transformation. The experiments found evidence for two new phases under pressure. In these two phases the electrical conductivity and the thermoelectric power were measured as functions of temperature and

pressure. The results, interpreted in terms of energy bands and deep-lying impurity levels, indicate that large changes in mobilities and state densities occur in transforming from one phase to another. Calculations suggest that this is associated with corresponding changes in the energy-band structure and width.

### EXPERIMENTAL TECHNIQUES AND OBSERVATIONS

High pressures were generated in Bridgman anvils. The technique is illustrated in Fig. 1. The sample is compressed by the hardened anvils and is contained by the Bridgman ring. The rings were made from an epoxide adhesive which provides an insulation resistance of over  $10^{13}$  ohms.<sup>5</sup> The stress system is not hydrostatic and therefore the sample undergoes a certain amount of shear deformation. We have minimized the non-hydrostatic effects by using a small sample diameter and by annealing the samples before making measurements. The results obtained are time-independent and are reversible with pressure. Pressure calibration of the system was made by observing the bismuth I-II and III-IV transitions.

The temperature of the sample was controlled by heaters placed behind each anvil. This arrangement allows one to adjust the temperature of the sample as well as to impose a desired temperature gradient. The temperature of each anvil flat was determined by a thermocouple placed directly in the high-pressure area of the anvil face.<sup>6</sup> For alumel-chromel thermocouples, used in this study, the effect of pressure on the thermoelectric emf is known to be small.<sup>7</sup> Experiments show that the temperature gradient over the face of the anvils is less than 3°C.

The sample emf produced by the temperature gradient was measured by using one side of each

\* The research reported in this paper was supported by the U. S. Office of Naval Research.

<sup>1</sup> O. H. LeBlanc, *J. Chem. Phys.* **35**, 1275 (1961).

<sup>2</sup> L. Friedman, *Phys. Rev.* **133**, A1668 (1964).

<sup>3</sup> P. E. Fielding and F. Gutman, *J. Chem. Phys.* **26**, 411 (1957).

<sup>4</sup> G. H. Heilmeyer and S. E. Harrison, *Phys. Rev.* **132**, 2010 (1963).

<sup>5</sup> R. J. Vaišnys and P. W. Montgomery, *Rev. Sci. Instr.* **35**, 985 (1964).

<sup>6</sup> R. S. Kirk and R. J. Vaišnys, *Science* **143**, 1436 (1964).

<sup>7</sup> F. P. Bundy, in *Progress in Very High Pressure Research*, edited by F. P. Bundy, W. R. Hibbard, and H. M. Strong (John Wiley & Sons, Inc., New York, 1961), p. 256.

thermocouple as a contact. The electrical resistance of the sample was computed from the applied voltage and the current through the sample. A Keithley 610A electrometer, used in conjunction with a Keithley 240 power supply, provided a range of voltages from under 10 mV to 1,000 V. A four-probe resistance measurement, performed by introducing additional voltage probes through the Bridgman ring, was made to check for deviations from Ohm's Law.

The Cu-Phth<sup>8</sup> was purified by a double sublimation at 550°C and the resulting crystals were identified by x-ray analysis to be in the  $\beta$  form.<sup>9</sup> The crystals were long, thin needles with the  $b$  axis being the largest dimension. When placed in the sample chamber there was a tendency to orient this axis parallel to the face of the anvil and therefore, at least until pressure induced transformations occur, the electrical measurements were performed more or less at right angles to the  $b$  axis.

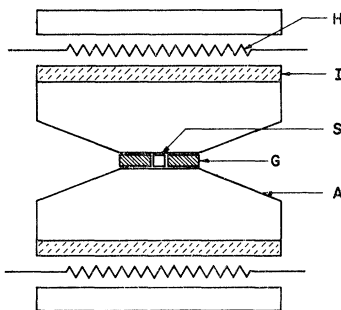


FIG. 1. Pressure assembly. The sample (S) is compressed by the anvils (A) and contained by the Bridgman ring (G). The temperature of the sample is adjusted by the heaters (H) and is measured by thermocouples placed at the sample-anvil junctions.

The electrical conductivity of Cu-Phth as a function of temperature can be described by the following equation:

$$\sigma = \sigma_0 e^{-E/kT}, \quad (1)$$

where  $E$  is an activation energy,  $k$  is Boltzmann's constant and  $T$  is the absolute temperature.  $\sigma_0$  is itself a function of temperature, but no independent determinations of the pre-exponential factor have been made and our measurements do not extend over a sufficient temperature range to define this dependence. We therefore treat  $\sigma_0$  as a constant. This procedure underestimates the true activation energy  $E_t$  as well as the pre-exponential factor  $\sigma_t$ , defined by the equation  $\sigma = \sigma_t e^{-E_t/kT}$  with  $\sigma_t = cT^{-n}$ . The terms of this equation are related to those of Eq. (1) by  $E_t = E + nkT_m$  and  $\sigma_t = e^n \sigma_0$ , where  $T_m$  is the mean temperature of the experiment. If, for example,  $n$  is taken as 2, a possible value for Cu-Phth, these corrections are appreciable.

The results of a typical measurement are shown in Fig. 2, where the logarithm of the resistance is plotted

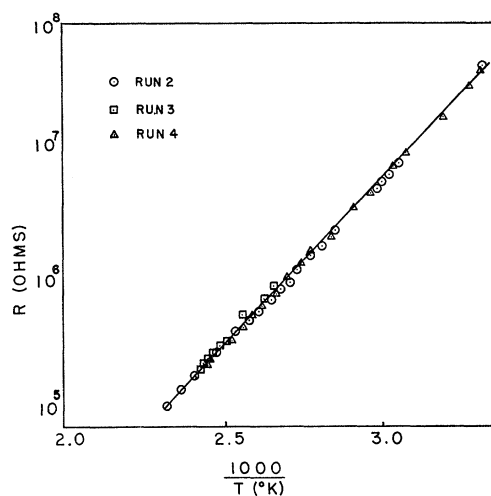


FIG. 2. The electrical resistance of Cu-Phth as a function of temperature at 30 kbar. The runs refer to different temperature cycles.

against the inverse temperature. Figure 3 shows the effect of pressure on the activation energy. The 1-atmosphere value was obtained before and after the specimens had been compressed. It is seen that at approximately 1–2 kbar the activation energy drops from 0.85 to 0.45 eV. In the pressure range 1 to 30 kbar the activation energy decreases at a rate of approximately  $3.3 \times 10^{-6}$  eV/bar. At 30 kbar there is a sudden increase in the activation energy from 0.35 to 0.55 eV. As the pressure is further increased the activation energy decreases at the rate of about  $2 \times 10^{-6}$  eV/bar. A typical thermoelectric power measurement is shown in Fig. 4 where the thermal emf produced by the temperature gradient is plotted against  $\Delta T$ . The behavior of the thermoelectric energy  $QT$  where  $Q = -dV/dT$ , at  $T = 320^\circ\text{K}$  is shown in Fig. 5 as a function of pressure. At about 1 kbar the thermoelectric energy is  $+0.37$  eV and it decreases at the rate of about  $2 \times 10^{-6}$  eV/bar with pressure. Between 50 and  $120^\circ\text{C}$ ,  $QT$  increases by 0.05 eV. At 30 kbar there is a sudden reversal of sign in the thermoelectric energy; it changes to about  $-0.30$  eV. As the pressure is increased,  $QT$  rises at the rate of about  $2 \times 10^{-6}$  eV/bar. In this pressure range,  $QT$  decreases by 0.02 eV in the temperature range 54 to  $110^\circ\text{C}$ .

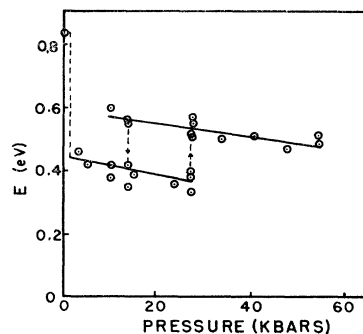


FIG. 3. The thermal activation energy for conduction in Cu-Phth as a function of pressure.

<sup>8</sup> Sample obtained from DuPont Company, Wilmington, Delaware.

<sup>9</sup> J. M. Robertson, J. Chem. Soc. (London) 1935, 615 (1935).

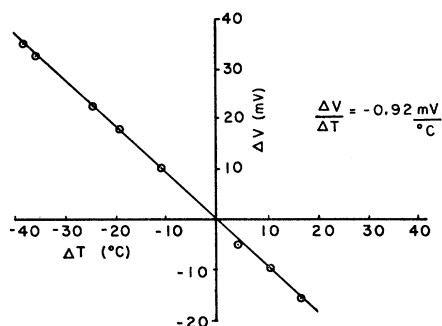


FIG. 4. The thermal emf of Cu-Phth as a function of the temperature difference across the sample. The mean temperature has been kept constant within  $5^{\circ}\text{C}$ .

The pre-exponential factor found in the study is approximately  $5\text{--}50 \text{ ohm}^{-1} \text{ cm}^{-1}$  in the  $\beta$  phase. At 1–2 kbar this decreases to about  $0.2 \text{ ohm}^{-1} \text{ cm}^{-1}$  and is approximately constant with pressure until 30 kbar. At this pressure the pre-exponential factor increases to about  $5 \text{ ohm}^{-1} \text{ cm}^{-1}$ .

Figure 6 shows the current-voltage behavior in a sample at 35 kbar. The current varies linearly with voltage up to an applied voltage of 600 V, corresponding to a field of  $3 \times 10^4 \text{ V/cm}$ . At higher fields the current increases more rapidly with the applied voltage. At the same pressure four-probe measurements with about 10 V across the sample show that Ohm's Law is satisfied.

The error in the thermoelectric power measurements due to the temperature uncertainty is less than 5%. In the activation energy determinations this error is probably under 3%. The uncertainties in the pressure from sample to sample are about 6 kbar and account for most of the scatter in  $E$  and  $QT$  as functions of pressure. In a given sample any pressure point may be reproduced to within a few percent. The pre-exponential factor is least precise of all our measurements, and is uncertain within a factor of 5; the accuracy is probably within a factor of 10. Finally, the temperature coefficient of  $QT$  is reliable to within about 50%. Certainly there is no question as to its sign.

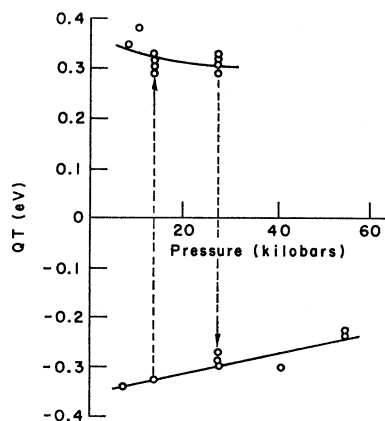


FIG. 5.  $QT$  for Cu-Phth as a function of pressure.

The discontinuities of the thermal activation energy  $E$ , of the thermoelectric energy  $QT$ , and of the resistance occur at the same pressure. We therefore identify these discontinuities with phase transformations occurring at about 1–2 and 30 kbar. These transformations are reversible with hysteresis. This can be seen in Figs. 3 and 5 where a certain amount of super-pressuring or under-pressuring occur. This behavior is common in solid-solid transformations under pressure. The lowest transformation occurs at a pressure which is below the accurate working limit of our apparatus and therefore we observe it only upon its completion. In the following discussion we will describe the region from 1 to 30 kbar as phase I, and above 30 kbar as phase II. The results of our measurements are summarized in Table I.

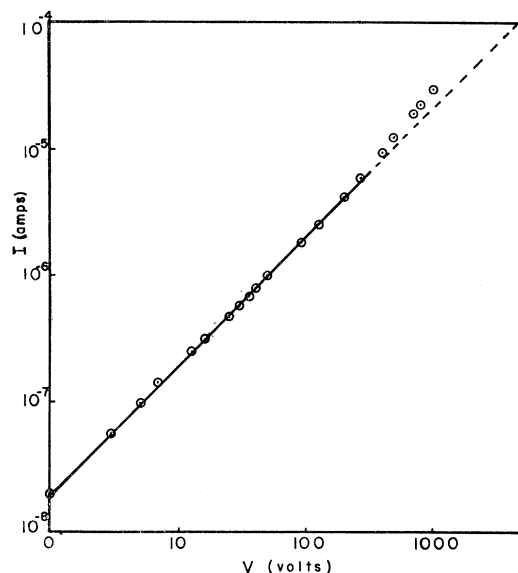


FIG. 6. The current as a function of applied voltage in a Cu-Phth sample at 35 kbar.

X-ray diffraction patterns were made at one atmosphere on samples before and after compression. The  $\beta$  crystal form was always observed. If the samples were subjected to a sudden decompression there was a distinct broadening of the diffraction lines. However, these lines sharpened if the samples were annealed at a low pressure before the pressure was entirely removed. This agrees with the hypothesis that there is at least one phase transformation under pressure. These experiments also eliminate the possibility that the high-pressure forms correspond to the  $\alpha$  phase, since this form should be recoverable under these conditions.<sup>10</sup>

The activation energy measured by us for the  $\beta$  phase agrees with the results for single crystals at one atmosphere obtained by other investigators<sup>3,4</sup>;  $0.85 \pm 0.05 \text{ eV}$ . Heilmeyer and Harrison<sup>4</sup> reported observations in which

<sup>10</sup> FIAT Final Report 1313, PB 85172 (1948), U. S. Department of Commerce, Vol. III, pp. 446–8, 462.

TABLE I. Experimental results for Cu-Phth under pressure.

Phase	$P$ (kbar)	$E$ (eV)	$QT^a$ (eV)	$\sigma_0/e^b$ ( $\text{cm}^{-1} \text{V}^{-1} \text{sec}^{-1}$ )	$dE/dP$ (eV bar $^{-1}$ )	$d(QT)/dP$ (eV bar $^{-1}$ )	$d(QT)/dT$ (eV deg C $^{-1}$ )
$\beta$	0.001	0.85	...	$3 \times 10^{19}$	...	...	...
PI	10	0.41	+0.35	$1 \times 10^{18}$	$-3.3 \times 10^{-6}$	$-2 \times 10^{-6}$	$+1 \times 10^{-3}$
PII	30	0.55	-0.30	$3 \times 10^{19}$	$-2 \times 10^{-6}$	$+2 \times 10^{-6}$	$-0.4 \times 10^{-3}$

<sup>a</sup> At 320°K.

<sup>b</sup> Uncorrected for the temperature dependence of  $\mu$  or  $E_f$ ;  $\sigma_0/e = (\mu N)_{\text{avg}}$ .

the activation energy changed from 0.83 eV below 390°K to 1.0 eV above this temperature. They interpret this upper temperature range as corresponding to intrinsic conduction and therefore they suggest that the value of  $E=0.85$  eV is associated with an impurity level at 1.7 eV from one of the bands. Our value of the pre-exponential factor in the  $\beta$  phase, 5–50  $\text{ohm}^{-1} \text{cm}^{-1}$ , may be compared with the one atmosphere measurements of Fielding and Gutman<sup>3</sup> on single crystals, where they find 30–350  $\text{ohm}^{-1} \text{cm}^{-1}$ . Heilmeier and Harrison<sup>4</sup> do not give directly the value of the pre-exponential factor, but it may be estimated from their geometry and seems to be lower than 30  $\text{ohm}^{-1} \text{cm}^{-1}$ .

Bradley, Grace, and Munro<sup>11</sup> have measured the effect of pressure on the activation energy and resistance of Cu-Phth. They find an activation energy of 0.55 eV at 30 kbar with a pressure coefficient about  $-2 \times 10^{-6}$  eV/bar. This corresponds closely to our observations in region II. Their pre-exponential factor, however, is 50 times lower than that found in this study. The discrepancy may arise because different pressure- and temperature-generating and cycling techniques were used; such factors are important when dealing with phase transformations under pressure. They do not report any activation energy which corresponds to our phase I.

### ANALYSIS OF RESULTS

The basic parameters characterizing the electrical properties of Cu-Phth are not well known even at 1 atmosphere. Only very approximate estimates can be made of the energy gap, state densities, mobilities, and impurity concentrations. It is therefore necessary to start our analysis with a general model and to fix the specific parameters by comparing the deductions of the model with the results of the experiments.

We assume that the band model is applicable and specialize it to deep lying acceptor and donor states (or equivalently shallow-trap states). The use of the band approach is justified since it seems to be applicable to other organic crystals<sup>1,12</sup> with larger energy gaps and weaker interactions than those found in Cu-Phth. As

will be seen, the band approach is consistent with our experimental observations as well. With regard to states within the energy gap, it is probable that they arise from organic impurities which are similar to Cu-Phth; inorganic materials are highly insoluble in most organic compounds and are virtually eliminated by sublimation because of the large difference in vapor pressures. Since the energy levels and mechanisms of charge separation in the organic impurities are similar to those in Cu-Phth itself, the donor levels should be close to the valence band and the acceptor levels to the conduction band. Finally, imperfections may be introduced by the action of the nonhydrostatic stress components. However, since molecular interactions are weak, such levels will be located within  $W_0$  of the band edge, where  $W_0$  is the band width of the conduction or valence band.

Let us consider a system having four energy levels  $E_l$  with corresponding state densities  $N_l$ , where  $l$  refers to holes ( $h$ ), donors ( $d$ ), acceptors ( $a$ ), or electrons ( $e$ ). At any temperature, if the distance of the Fermi level from a given energy level is more than a few  $kT_m$ , and if a narrow transition range is neglected, the position of the Fermi level is determined by two of the above states. Let these states be  $i$  and  $j$ , such that  $E_i < E_f < E_j$  ( $i=h, d$ ;  $j=e, a$ ; the inequality expresses the deep-level condition). Which states are important in a given case is determined by requiring over-all crystal neutrality. The location of the Fermi level relative to the valence band (i.e.,  $E_h(T) \equiv 0$ ) is then given by

$$E_f = \frac{1}{2}(E_i + E_j) + \frac{1}{2}(kT) \ln(N_i/N_j). \quad (2)$$

$E_i$  and  $E_j$  may depend on the temperature. For a small temperature range,  $(E_i + E_j)$  may be expressed in terms of the slope (evaluated at  $T_m$ ) and the intercept (evaluated at  $T=0$ ) of the tangent to the  $(E_i + E_j)$ -versus- $T$  curve. Thus  $(E_i + E_j) = (E_i + E_j)^0 + 2\gamma T$ , where  $2\gamma = d(E_i + E_j)/dT \approx d(E_e + E_h)/dT$ . (The assumption that  $\gamma$  is about the same for both impurities and band edges is known to be valid for several wide band semiconductors<sup>13</sup>; it is probably even a better approximation in our case because the appropriate impurity and band levels are so closely related. The analysis presented below does not require this assumption. In the final results, a different assumption on this point would yield somewhat different mobility and impurity density

<sup>11</sup> P. S. Bradley, J. D. Grace, and D. C. Munro, in *The Physics and Chemistry of High Pressures* (Society of Chemical Industries, London, 1963), p. 143.

<sup>12</sup> R. G. Kepler in *Organic Semiconductor Conference*, edited by J. J. Brophy and J. W. Buttrey (The Macmillan Company, New York, 1962), p. 1.

<sup>13</sup> W. Paul, *J. Phys. Chem. Solids* **8**, 196 (1959).

ratios.) In general  $E_f$  is not equal to  $\frac{1}{2}E_g$  (where  $E_g = E_e^0 + E_h^0$ ) even if  $i=h$  and  $j=e$ . The conductivity of the sample may be expressed as the sum of hole and electron contributions,  $\sigma = \sigma_h + \sigma_e$ , and with the previously defined Fermi level the individual conductivities are given by

$$\sigma_e = e\mu_e N_e (N_j/N_i)^{1/2} e^{-\gamma/k} e^{-[E_g - (E_i + E_j)^0]/2kT} \equiv \sigma_{0e} e^{-E_e/kT}, \quad (3)$$

$$\sigma_h = e\mu_h N_h (N_j/N_i)^{1/2} e^{-\gamma/k} e^{-(E_i + E_j)^0/2kT} \equiv \sigma_{0h} e^{-E_v/kT}. \quad (4)$$

It is convenient to define the ratio of electron to hole conductivities as

$$r = \sigma_e/\sigma_h = (\mu_e N_e N_i / \mu_h N_h N_j) e^{-[E_g - (E_i + E_j)^0]/kT} \equiv r_0 e^{-\Delta/kT}. \quad (5)$$

The terms  $E_e$ ,  $E_v$ ,  $\Delta$ ,  $\sigma_{0e}$ ,  $\sigma_{0h}$ , and  $r_0$  are defined by the equivalence relations in Eqs. (3)–(5). The conductivity is electron dominated if  $r > 1$ , and for  $r < 1$  the conductivity is dominated by holes. We observe that in general  $r$  will depend upon the temperature. The thermoelectric power may be also expressed as the sum of electron and hole contributions,  $Q = (\sigma_e Q_e + \sigma_h Q_h)/\sigma = (rQ_e + Q_h)/(1+r)$ , with the individual terms being given by

$$Q_e = -[E_e + \frac{1}{2}(kT) \ln(N_j/N_i) + \gamma T + \eta T]/T, \quad (6)$$

$$Q_h = [E_v - \frac{1}{2}(kT) \ln(N_j/N_i) + \gamma T + \eta T]/T. \quad (7)$$

$\eta T$  is the kinetic energy contribution of the carriers, assumed to be the same for both bands. Finally the temperature derivative of  $QT$  is given by

$$d(QT)/dT = [r(E_e/T + Q_e) - (E_v/T - Q_h)]/(1+r) + r(\Delta/kT)(Q_e - Q_h)/(1+r)^2. \quad (8)$$

We proceed to compare the experimental results with the above theoretical deductions. We first note that if within the temperature range of the investigation  $r$  passes through the value 1, the nature of the dominant carrier will change. Thus a plot of  $\ln\sigma$  versus  $1/T$  will show two regions with different activation energies. Since we see only a single activation energy in our experiments one of the following must be applicable: either  $r$  is a constant, independent of temperature, or else  $r$  is temperature dependent but always lies either above or below 1 in the experimental temperature range.

We first consider the special, limiting case of  $r$  a constant (i.e.,  $\Delta=0$ ). Then the last term of Eq. (8) vanishes and the thermoelectric energy may be written as

$$QT = (E + \gamma T + \eta T)[(1-r)/(1+r)] + \frac{1}{2}(kT) \ln(N_i/N_j).$$

Extrapolation of this expression to absolute zero is a convenient method for evaluating  $r$ ; in our case it is found that  $r=0.5$  in phase I and  $r=1.3$  in phase II when the appropriate experimental and estimated (see below) parameters are used.

Unfortunately, there is no *a priori* reason for assuming that  $r$  is constant and therefore the temperature-dependent case must be considered. If  $r > 50$ , then use of Eqs. (3)–(6) gives the relationship  $d(Q_e T)/dT = (E + Q_e T)/T$ ; that is,  $QT$  and its temperature derivative should have opposite signs when  $E > |QT|$  (since  $Q_e T$  is negative, but the term  $(E + Q_e T)/T$  is positive). Inspection of Table I shows for phase II, where the thermoelectric power is electron dominated and  $E > |QT|$ , that  $QT$  and  $d(QT)/dT$  have the same sign in this phase. Therefore  $r$  must be less than 50 in this phase if  $r$  is temperature-dependent. Similarly, the use of Eqs. (3)–(5), (7) leads to the results that  $(dQ_h T)/dT = -(E - Q_h T)/T$  if  $r < 0.02$ , and by an analogous argument it is concluded that  $r$  must be greater than 0.02 in phase I if it is temperature-dependent. The examination of the general range of  $r$  is made difficult by the nonlinear appearance of  $r$  in the expressions for  $QT$ ,  $d(QT)/dT$ , and  $E$ . Further, some of the restrictions on  $r$ , arising from the experimental determinations of the above quantities, are difficult to express and manipulate analytically. For these reasons the possible variation of  $r$  was examined numerically with an IBM 7094 computer. Both  $r_0$  and  $\Delta$  were varied; the former between approximately  $10^{-4}$  and  $10^4$  and the latter between  $-0.6$  and  $+0.6$  eV. The variations were subject to the condition that  $r$  must always be either less than or greater than one over the experimental temperature range. The calculations were performed with estimated values of  $\gamma$  and  $\eta$  (see below) and with a range of  $10^4$  and  $0.4$  eV in the values of  $N_i/N_j$  and  $E_g$ , respectively; the results are quite insensitive to errors in these estimates. An error of 10% was allowed in  $E$ . The analysis leads to the following conclusions consistent with the experimental observations: In phase I,  $r$  may vary between 0.6 and 0.3 as  $\Delta$  varies between 0 and  $-0.05$  eV; the corresponding range in  $r_0$  is between 0.6 and 0.06. In phase II,  $r$  may be between 1.3 and 3 while  $\Delta$  may correspondingly vary between 0 and 0.05 eV. This corresponds to a range of 1.3 to 15 in  $r_0$ . When  $\Delta=0$ , we have the limiting case of a temperature independent  $r$  treated initially, above.

We conclude that the experimental activation energy is related to the energy gap by  $E_g = 2E$  with a maximum uncertainty of 0.05 eV. Further,  $r$  cannot be strongly temperature-dependent and there is no doubt that the nature of the dominant carriers is reversed in the course of the phase transformation I-II.

The temperature coefficient of  $QT$  provides a relationship among  $\eta$ ,  $\gamma$  and  $N_i/N_j$ . The mobilities and band state densities are related to these quantities through the pre-exponential term. To proceed further with the analysis we must determine or estimate the permissible range of the above variables. It must be pointed out that the uncertainties inherent in this procedure are large since in general these variables are related exponentially to the experimentally measured quantities.

The value of  $\gamma$  may be determined by assuming that the energy gap is a function only of the volume,

$$\gamma = dE_f/dT \approx dE/dT \approx -(\alpha/\beta)dE/dP, \quad (9)$$

where  $\alpha$  is the coefficient of thermal expansion and  $\beta$  is the compressibility. The value of  $dE/dP$  is given by our measurements. The compressibility is not known for Cu-Phth but the ratio  $(\alpha/\beta)$  should be about the same for similar organic substances and we use  $(\alpha/\beta) = 10^2$  bars/°C.<sup>14</sup> To a first approximation this ratio is pressure-independent. With these assumptions,  $\gamma = 3k$  in phase I and  $\gamma = 2k$  in phase II. These estimates are probably valid within a factor of 2, but since they appear as exponents in the conductivity expression this leads to considerable uncertainty in the actual modification of pre-exponential term.

To estimate  $\mu$ ,  $N$ , and  $\eta$  it is convenient to treat the narrow-band and wide-band cases separately. For a wide band ( $W_0 > kT_m$ ), to a first approximation, the mobility is given by  $\mu = e\tau/m^*$ , where the effective mass is denoted by  $m^*$ . The uncertainty principle sets a lower limit on the relaxation time,  $\tau$ , of  $\hbar/W_0$  and the effective mass is approximately given by  $\hbar^2/a^2W_0$ , where  $a$  is the lattice constant. If  $W_0 \approx 10kT_m$ , then  $\mu \geq 1$  cm<sup>2</sup>/V sec; the corresponding density of states,  $N$ , is about  $10^{20}$  cm<sup>-3</sup>. Thus, the expected intrinsic pre-exponential factor,  $\mu N$ , is  $10^{20}$  or greater. In this case  $\eta$ , while it depends to some extent upon the scattering mechanism, is expected to be about  $2k$ .

If the band is narrow ( $W_0 < kT_m$ ), then all the energy states are accessible to the carriers and the appropriate density of states is approximately the density of molecules, about  $10^{21}$  cm<sup>-3</sup>. The uncertainty principle again sets a lower limit on the relaxation time of  $\hbar/W_0$ , but here this  $\tau$  corresponds to a mobility of  $\mu \geq 0.1 W_0/kT$  cm<sup>2</sup>/V sec.<sup>2,15</sup> Thus for a bandwidth of  $kT_m$  the intrinsic pre-exponential factor is again given by  $\mu N \geq 10^{20}$ . While in principle the pre-exponential factor may be made arbitrarily small by making the bandwidth sufficiently narrow, the band approach is hardly applicable if the bandwidth is much less than  $kT_m$ . It may be noted that the experimentally observed mobilities in anthracene and naphthalene are of the order of unity.<sup>12,16</sup> For a narrow band, approximately,  $\eta$  is reduced by a factor of the order of  $W_0/kT_m$  from its wide band value, as indicated by Friedman.<sup>2</sup>

The sublimation procedure used in this work probably lowers the concentration of even organic impurities to less than 1%. This corresponds to an upper limit of  $10^{19}$  cm<sup>-3</sup> for donors or acceptors, and is a reasonable

estimate of the upper limit of defects introduced by strain as well.

We return to the consideration of the temperature coefficient of  $QT$ . If we take  $5k$  and  $4k$  for  $\gamma + \eta$  in phases I and II, respectively, and use the observed temperature coefficients of  $QT$ , we find that  $N_i/N_j = 10^5$  (with a range of  $10^2 - 10^8$ ) in phase I and  $N_i/N_j = 10^{-5}$  (range  $10^{-2} - 10^{-8}$ ) in phase II. If smaller values are used for  $\gamma + \eta$  then the ratios deviate more from unity.

At this point we can attempt to identify  $i$  and  $j$ . We first note that the ratio  $N_i/N_j$  has been inverted in going through the phase transformation I-II. This means that  $i$  and  $j$  can not refer simultaneously to donors and acceptors, respectively (unless we allow several classes of donors or acceptors). On the other hand,  $i$  and  $j$  may refer to the valence and conduction bands. This interpretation requires that the conduction band broaden, and the valence band narrow, in the phase change I to II. For a given band, a change of a factor of  $10^3$  is conceivable if the band changes from a very narrow one to a rather broad one in the course of the pressure transformation. Similarly,  $i$  and  $j$  may be identified with the valence band and acceptor levels in phase I, and with the donor levels and the conduction band in phase II, respectively. This requires, for example, that the donor levels be absorbed into the valence band in phase I. In both cases only the values of  $N_i/N_j$  closest to unity (in the ranges given) are reasonable because the activation energy is known to be identical with  $\frac{1}{2}E_g$  within at most  $2kT_m$ .

If  $(i, j) = (h, e)$ , that is the determining levels are the hole and electron bands, we observe that  $r = \mu_e/\mu_h$ . The observed increase of  $\sigma_0$  in the I-II transition may be due to either increases in the mobilities and/or changes in the mean state densities. What is surprising, however, is that apparently such large changes in the ratio of band densities (at least a factor of  $10^4$  in the density ratio) are accompanied by much milder changes in the mobility ratio (at most a factor of 300, and possibly only a factor of 2). The most likely explanation is that the mobility is in fact defect (trap) limited in the high pressure forms. This is not at all surprising since  $\beta$  Cu-Phth is known to have a high trap density.<sup>17</sup> Such an assumption can be used to explain our observed current voltage nonlinearities as well. The observed  $\sigma_0$ 's, after account is taken of the terms which arise from the temperature dependence of  $\mu$  and  $E_f$ , are consistent with the uncertainty principle. In form II, the carrier mobility calculated from  $\sigma_0$  is at least 10 times the minimum value since it is very unlikely that both  $\mu$  and  $N$  would increase at the same time.

On the other hand if  $(i, j)$  are identified with  $(h, a)$  in form I and with  $(d, e)$  in form II, and if we take  $N_i/N_j = 10^2$ , (phase I), we note that  $(\mu_e N_e/\mu_h^2 N_h) = r(N_j/N_i) \approx 10^{-2}$  in form I and  $10^{+2}$  in form II. If

<sup>14</sup> E. F. Westrum, Jr., and J. P. McCullough in *Physics and Chemistry of the Organic Solid State*, edited by D. Fox, M. M. Labes, and A. Weissberger (John Wiley & Sons, Inc., New York, 1963), Vol. 1, p. 1.

<sup>15</sup> H. Fröhlich and G. L. Sewell, Proc. Phys. Soc. (London) **74**, 643 (1959).

<sup>16</sup> M. Silver, J. R. Rho, D. Olness, and R. C. Jarnagin, J. Phys. Chem. **38**, 3030 (1963).

<sup>17</sup> G. H. Heilmeyer and G. Warfield, J. Chem. Phys. **38**, 163 (1963).

we make the plausible assumption that the geometric mean of the state densities is the same in both phases and the  $(N_a)_I = (N_a)_{II}$  (where the subscripts denote the pressure forms), and use the experimental pre-exponential factors, we find that  $(\mu_h/\mu_e)_I \approx (\mu_e/\mu_h)_{II}$ ; that is the mobility ratio is inverted in the I-II transformation. Further, we calculate from  $\sigma_0$  that the more mobile carriers in phase I have a mobility of 10 times, and in phase II a mobility of 100 times that given by the uncertainty principle argument (if the density of states is taken to be  $10^{20}$ – $10^{21}$  cm $^{-3}$ , as estimated above). This implies, for example, an electron mobility of 10–100 cm $^2$ /V sec in phase II of Cu-Phth.

The above analysis then leads to the following conclusions for phases I and II. The activation energy  $E$  is directly related to the energy gap,  $E = \frac{1}{2}E_g$ . The mobility of the most mobile carriers in each phase is at least 1 cm $^2$ /V sec, and it may be as high as 100 cm $^2$ /V sec in phase II. Structural changes under pressure are accompanied by reversals of sign of the dominant carrier. The experiments indicate that these changes are accompanied by order of magnitude changes in both the mobilities and the state densities.

It is not possible to decide whether the material is chemically intrinsic or not. However, if imperfections are present, they are concentrated and contribute deep impurity (or shallow defect) levels, within a few  $kT_m$  of the band edges. If the material is intrinsic, carrier mobility may be defect limited.

### MODEL CALCULATIONS

The experimental results indicate that pressure produces two effects on Cu-Phth. First there is a continuous decrease in the energy gap as might be expected from an increase in molecular interactions. Secondly, there are discontinuous changes, both increases and decreases, in the energy gaps, the mobilities and the densities of state. Since Cu-Phth has three known crystal forms at atmospheric pressure,<sup>18</sup> the production of two new phases under high pressure would not be unusual. Indeed optical experiments<sup>19</sup> have shown that Cu-Phth undergoes a phase transformation at a pressure somewhat below 20 kbar; the experimental circumstances make it difficult to correlate at present the optical observations with the electrical work, but it is probable that the high-pressure form is phase II. Examination of the morphological changes in the crystals suggests that the transformation is from the  $\beta$  form to the structure normally found in platinum phthalocyanine<sup>20</sup> at 1 atmosphere. Such a transformation essentially involves a reorientation of the phthalocyanine molecules along the  $b$  axis. The two structures are indicated in Fig. 7. Such a rearrangement would

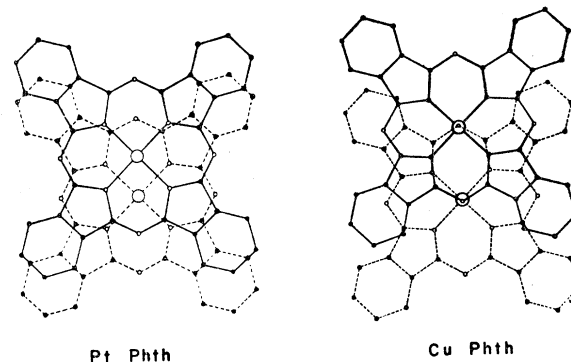


Fig. 7. The structures of Cu- and Pt-phthalocyanine (after Robertson, see Refs. 19 and 20).  $\circ$  = Cu, Pt;  $\bullet$  = C;  $\circ$  = N.

tend to increase the overlap between the Cu-Phth molecules and to strengthen the molecular interactions. In electrical measurements such rearrangements would be manifest as changes in the energy gap and carrier mobility. But these changes need not be simple, since the bandwidth is sensitive to the symmetry as well as the magnitude of the interaction.

To examine these points in more detail we have made tight binding calculations of effects of pressure on the bandwidth in a crystal, both through compression and through induced phase changes. The crystals were constructed from anthracene molecules, since the molecular orbitals of Cu-Phth are not available.

This calculation can not be expected to give quantitative results but it should suggest the relative importance of different factors. The calculated energies should be smaller than the experimental ones since the nearest-neighbor tight-binding method intrinsically underestimates the total interaction. Further, the presence of the nitrogen and metal atoms in the Cu-Phth would accentuate the effects of structure. Indeed, since some of the observed energy gap changes in Cu-Phth are large, the tight-binding method may be inadequate; in addition there is the possibility that new molecular levels, below those involved in band formation in the  $\beta$  phase, may become important at high pressure. The crystal structures, used in the calculations, shown in Fig. 8, are similar to the two phthalocyanine structures (Fig. 7) and also correspond to the crystal forms of several large condensed ring compounds.<sup>21</sup> The method of calculation is similar to that employed by LeBlanc<sup>1</sup> in calculating the band structure of anthracene. The crystal wave functions are constructed from molecular orbitals  $\varphi(r)$ , which in turn are Hückel combinations of carbon  $2p$  state orbitals. Under these circumstances the energy of an extra electron or hole in the crystal is given by

$$E = E_0 + E_1 + \sum_l E_2 e^{i\mathbf{k}\cdot\mathbf{l}}, \quad (10)$$

where  $E_1 = \int \varphi^*(\mathbf{r}) V(\mathbf{r}+\mathbf{l}) \varphi(\mathbf{r}) d\mathbf{r}$  and  $E_2 = \int \varphi^*(\mathbf{r}+\mathbf{l})$

<sup>18</sup> J. W. Eastes, (to American Cyanamid Co.), U. S. Patent 2,770,629 (1956).

<sup>19</sup> J. R. Vaišnys and R. S. Kirk (to be published).

<sup>20</sup> J. M. Robertson, J. Chem. Soc. (London) 1940, 36 (1940).

<sup>21</sup> J. M. Robertson, J. Chem. Soc. (London) 1937, 219 (1937).

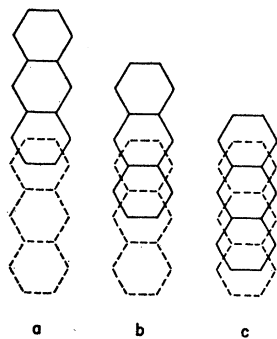


FIG. 8. The three hypothetical structures used in the model calculations. The molecules shown are related by translation in the  $b$  direction. Projection normal to molecular plane.

$\times V(\mathbf{r}+\mathbf{l})\varphi(\mathbf{r})d\mathbf{r}$  and  $\mathbf{l}$  refers to nearest neighbors.  $E_1$  gives the average shift of the molecular levels due to the neighboring molecules. In this approximation  $E_1$  is the same for both holes and electrons; it provides a convenient measure of molecular interactions at different pressures.  $E_2$  is a measure of the bandwidth. The evaluation of the bandwidths was performed for the  $b$  direction since this is the direction of largest molecular interaction and nearest neighbors in other directions contribute less than 2% to the results. The results of the calculations for the different structures are shown in Table II. The effects of compressing the crystals in

TABLE II. Results of tight-binding calculations of the bandwidth and average band-shift terms for different crystal structures and compressions.

Structure	$E_{2(e)}$ ( $\times 10^{-15}$ erg)	$E_{2(h)}$ ( $\times 10^{-15}$ erg)	$E_1$ ( $\times 10^{-15}$ erg)
a (normal)	70	27	4
(compressed)	309	49	28
b (normal)	35	76	10
(compressed)	122	129	39
c (normal)	3	26	14
(compressed)	44	37	82

the  $b$  direction by 15% are also shown. This compression corresponds to an applied pressure of 100–150 kbars.

Changes in structure, as indicated in Fig. 8 and Table II, increase the overlap of molecules in the  $b$  direction and hence produce an increase in  $E_1$ . Qualitatively, this is the expected result. The corresponding changes in the bandwidths are larger but much less regular. It is clear that structural changes can reverse the sign of the dominant carriers (e.g., transformation  $a$ - $b$ ) as well as produce marked changes in the mobilities and state densities; in narrow bands, for example,  $\mu$  is proportional to  $E_2$ . The effects on transport properties are accentuated<sup>2</sup> when  $W_0$  is less than  $kT_m$ . In passing it may be noted that the extremely narrow bandwidth for electrons in structure  $c$  arises in much the same way as the narrow electron band in the  $c$  direction of anthracene found by LeBlanc.<sup>1</sup>

For the three structures under consideration it is seen that simple compression increases the molecular

interactions, producing increases in the average band energy and the bandwidth. (Since the bandwidth involves the partial cancellation of terms, the opposite pressure effect could be observed under certain circumstances.) Pressure can broaden the bandwidth by more than a factor of 10. A change of this kind would have a large effect on the mobility and the state density. In addition, the rate at which pressure affects the bands can be quite different in the two bands so that pressure may reverse the nature of the dominant carriers (e.g., structure  $c$ ).

Within the tight-binding approximation changes in the energy gap correspond to changes in the mean of the electron and hole bandwidths. The calculated pressure derivatives of the activation energy range from  $-0.4 \times 10^{-6}$  eV/bar in structure  $a$  to  $-0.1 \times 10^{-6}$  eV/bar in structure  $c$ . These values are less than, but of a similar magnitude to those found experimentally. The calculated changes in  $E$  due to structure changes are between  $4 \times 10^{-2}$  and  $4 \times 10^{-3}$  eV; the ratio of these values to the experimental ones is about the same as the ratio of theoretical and experimental pressure derivatives.

The effect of compression and structure transformation on impurity levels is measured approximately by the term  $E_1$ . Since  $E_2$  is more sensitive to pressure it is expected that deep donor and acceptor levels will be absorbed by the corresponding bands as the bands broaden. Thus even with large concentrations of deep impurities, pressure could produce intrinsic semiconduction.

## CONCLUSION

In this paper we have described an investigation of the electrical properties of copper phthalocyanine, with pressure as the important variable. We have described a versatile technique which can generate significant information about charge transport in weakly interacting systems. In addition to providing a characterization of copper phthalocyanine, the experimental results, in considerable detail, are found to be consistent with the band model of the solid and indicate that this approach is appropriate for molecular systems at high pressure. It is found that pressure has a continuous but relatively minor effect on energy gaps, mobilities, and state densities; pressure-induced phase transformations however change the latter two parameters by several orders. These results, as well as theoretical considerations, suggest that the bandwidth can be quite sensitive to the relative phase of the molecular wave functions. Structure may therefore provide effective means of modifying the electrical properties of this class of compounds.

## ACKNOWLEDGMENT

The financial support of the U. S. Office of Naval Research is gratefully acknowledged.